Jahn-Teller distortions as a novel source of multiferroicity

Paolo Barone,[1] Kunihiko Yamauchi,[2] and Silvia Picozzi[1]
[1]*Consiglio Nazionale delle Ricerche (CNR-SPIN), 67100 L'Aquila, Italy*
[2]*ISIR-SANKEN, Osaka University, 8-1 Mihogaoka, Ibaraki, Osaka 567-0047, Japan*
(Received 30 January 2015; published 27 July 2015)

The Jahn-Teller effect is a fascinating and ubiquitous phenomenon in modern quantum physics and chemistry. We propose a class of oxides with a melilite structure $Ba_2TGe_2O_7$ (T = V,Ni) where Jahn-Teller distortions are mainly responsible for the appearance of electric polarization. At the heart of the proposed mechanism lies the lack of inversion symmetry displayed by tetrahedrally coordinated transition-metal ions, which allows for the condensation of polar Jahn-Teller distortions, at odds with octahedral coordination typical of conventional ferroelectric oxides with a perovskite structure. Since the noncentrosymmetric local environment of transition-metal ions also activates the proposed spin-dependent hybridization mechanism for magnetically induced electric polarization, proper multiferroic phases with intrinsic magnetoelectric interactions could be realized in this class of low-symmetry materials.

DOI: 10.1103/PhysRevB.92.014116 PACS number(s): 77.80.−e, 71.70.Ej, 75.85.+t

I. INTRODUCTION

Jahn-Teller (JT) distortions represent a universal mechanism by which spontaneous symmetry breaking may occur in condensed-matter systems. Colossal magnetoresistance in manganites has been explained invoking the essential role of the Jahn-Teller effect [1], which has been also invoked in several high-temperature oxide and fullerene superconductors [2,3]. Even though JT distortions are nonpolar in the perovskite ABO_3 structure displayed by many ferroelectric oxides, the ferroelectric transition in these systems has been also explained in terms of a pseudo Jahn-Teller (PJT) instability which can take place whenever the vibronic coupling between the ground and excited states is sufficiently strong [4]. The cooperative PJT effect in ferroelectrics has been known for a long time, nevertheless, its possible realization in multiferroic perovskite oxides, showing the simultaneous presence of magnetic and ferroelectric ordering, has been only recently suggested [5–8]. Interestingly, such a mechanism defies the empirical exclusion rule, according to which proper ferroelectricity and magnetism should be chemically incompatible and mutually exclusive [9].

On the other hand, the quest for sizable magnetoelectric (ME) effects has been pursued in the last decade mainly among magnetically induced improper ferroelectrics, where the microscopic ME interaction is expected to be intrinsically large. In this respect, a very interesting class of materials recently has been the object of intense research activity, suggesting a local origin of ME coupling in low-symmetry crystals through a spin-dependent hybridization mechanism [10–15]. Essentially, the lack of inversion symmetry in the point group of transition-metal ions may drive the appearance of local dipoles via an anisotropic hybridization, modulated by the atomic spin-orbit coupling, between the transition-metal ions and the surrounding oxygens. Materials belonging to the melilite family, with a general formula $A_2TB_2O_7$ (A^{+2} alkaline metal, T^{+2} transition metal, B^{+2} = Si,Ge), consisting of B_2O_7 dimers linked by TO_4 tetrahedra, represent an interesting playground, where the local properties of T^{+2} cations with tetrahedral coordination could be explored in detail. Among these, several compounds have been already synthesized, i.e., $Ba_2TGe_2O_7$ (T = Mn,Co,Cu) [12,16] and $A_2CoSi_2O_7$ (A = Sr,Ca) [17,18]. Due to the lack of inversion symmetry and to the quasi-two-dimensional (2D) character of their magnetic interactions, these materials have been predicted to host peculiar incommensurate magnetic spiral ordering [19] and skyrmion excitations [20], multiferroicity and highly nonlinear magnetoelectric responses [12,16,18,21], as well as magnetochiral [22] and giant directional dichroism in resonance with both electrically and magnetically active spin excitations [23]. The latter phenomena have been mostly explained in terms of the local ME interaction discussed above; specifically, the multiferroic phase observed in $Ba_2CoGe_2O_7$ has been shown to have an improper origin, the ferroelectric polarization being induced by the magnetic order.

In this respect, a possibility is to consider JT instabilities and a possible *proper ferroelectric transition* for T ions showing degenerate electronic states in tetrahedral symmetry. The lack of inversion symmetry of the local tetrahedral environment allows for odd ionic displacements to couple with the degenerate electronic states and, therefore, for the symmetry-allowed appearance of local dipole moments. In principle, this could imply proper multiferroicity with intrinsically large ME coupling in the family of melilite oxides. We notice that, despite the fact that the possible occurrence of polar JT distortions in crystals without a local center of inversion has been known for a long time and experimentally revealed, e.g., in rare-earth oxides (such as $DyVO_4$) or in praseodymium compounds (such as $PrCl_3$) [24–31], so far its relevance in the field of multiferroics has been overlooked. Based on these premises, we first discuss in Sec. II the Jahn-Teller problem relevant for the tetrahedral units TO_4 appearing in the melilite crystal. On the basis of general symmetry considerations, we show that polar JT distortions may locally develop in this structure when JT-active transition-metal ions are considered. Density functional theory (DFT) calculations are then used to propose melilite oxides where such polar JT effects can appear, possibly leading to ferroelectric, antiferroelectric, or ferrielectric phases, as discussed in Secs. III and IV.

 ©2015 American Physical Society

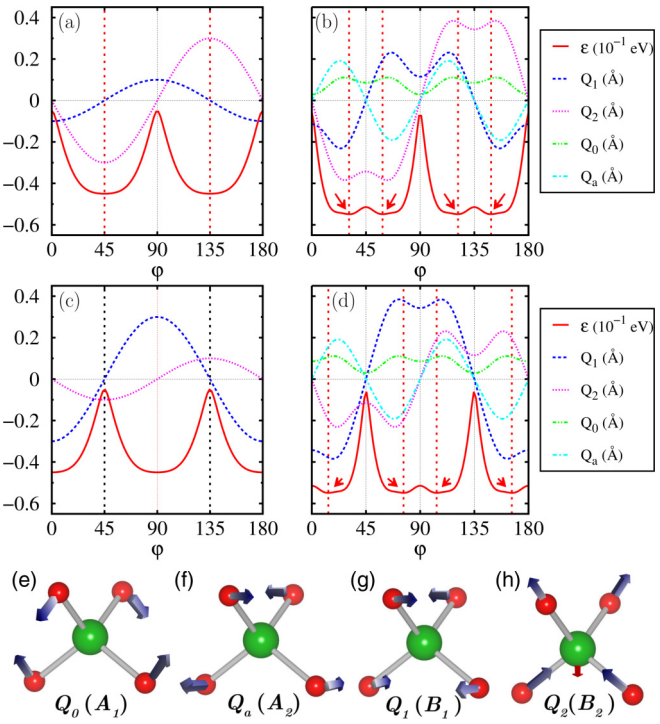

FIG. 1. (Color online) (a)–(d) Typical evolution of JT modes [shown in (e)–(h)] and energy as a function of the electronic angle φ for linear and quadratic couplings. The parameters have been chosen as $K_1 = K_2 = K_a/2 = K_0/2 = 1\ \mathrm{eV/\AA}^2, F_1 = 0.3(0.1)\ \mathrm{eV/\AA}, F_2 = 0.1(0.3)\ \mathrm{eV/\AA}$ in the top (bottom) panels, corresponding to cases a and b discussed in the main text. Quadratic coupling constants are set to zero in the left panels [(a), (c)], while $L_1 = L_2 = 0.9\ \mathrm{eV/\AA}^2$ and $G_1 = G_2 = 0.5\ \mathrm{eV/\AA}^2$ in right panels [(b), (d)]. Arrows and vertical lines highlight the energy minima. (c)–(f) Schematic representation of the symmetrized displacements in each tetrahedral unit, corresponding to totally symmetric displacements with symmetry (e) A_1 and (f) A_2, and to nontotally symmetric displacements with symmetry (g) B_1 and (h) B_2.

II. POLAR JAHN-TELLER EFFECT AT TETRAHEDRAL SITES OF MELILITE STRUCTURE

Due to the quasilayered structure of the melilite structure, each TO_4 appears to be slightly compressed along the c axis, thus belonging to the tetragonal D_{2d} group. As a consequence of the tetragonal crystal field, transition-metal d states are split into nondegenerate $d_{z^2}, d_{x^2-y^2}$, twofold d_{yz}, d_{zx}, and nondegenerate d_{xy} states. The corresponding Jahn-Teller problem for degenerate d_{yz}, d_{zx} is then expressed as $E \otimes (a_1 + a_2 + b_1 + b_2)$. By introducing the standard symmetrized displacements $Q_0(A_1), Q_a(A_2), Q_1(B_1)$, and $Q_2(B_2)$, describing totally and nontotally symmetric displacements shown in Figs. 1(e)–1(h), the vibronic matrix defined on the degenerate electronic states reads [4]

$$W = \begin{pmatrix} \Delta_1 & \Delta_2 \\ \Delta_2 & -\Delta_1 \end{pmatrix}, \tag{1}$$

where

$$\begin{aligned} \Delta_1 &= F_1 Q_1 + L_2 Q_a Q_2 + G_1 Q_1 Q_0, \\ \Delta_2 &= F_2 Q_2 + G_2 Q_0 Q_2 + L_1 Q_1 Q_a, \end{aligned} \tag{2}$$

including both linear F_1, F_2 and quadratic $G_i \equiv G(A_1 \times B_i), L_i \equiv G(A_2 \times B_i)$ couplings. Notice that the nontotally symmetric Q_1 and Q_2 modes describe a nonpolar and polar displacement, respectively, as highlighted in Figs. 1(g) and 1(h). Upon inclusion of the elastic term $H_0 = (1/2)\sum_i K_i Q_i^2$, the leading distortions as a function of all vibronic parameters can be obtained by minimizing the corresponding energy $\mathcal{E} = \frac{1}{2}\sum_i K_i Q_i^2 \pm \sqrt{\Delta_1^2 + \Delta_2^2}$. Analytical solutions are found only when the quadratic L_i couplings are neglected; however, all modes Q_i of the full JT problem can be obtained as a function of the stationary electronic states, namely, of the mixing angle φ through which the ground state is expressed as $|\psi\rangle = \cos\varphi|yz\rangle + \sin\varphi|zx\rangle$ [32].

When $L_i = 0$, two kinds of energy minima are found, where only one of the nontotally symmetric modes with B_1 and B_2 symmetry is activated, either $Q_1 = 0, Q_2 \neq 0$ or $Q_1 \neq 0, Q_2 = 0$, depending on the ratio between linear vibronic and elastic energies $K_2 F_1^2 \gtrless K_1 F_2^2$, as shown in Figs. 1(a) and 1(c) and later on labeled as case a and b, respectively [4]. In terms of the electronic wave functions, the two energy minima correspond to $\varphi_a = \pm\pi/4$ (case a) and $\varphi_b = 0, \pi$ (case b), i.e., to a symmetric mixing of d_{yz}, d_{zx} states or to split levels with d_{yz} or d_{zx} unique character, respectively. On the other hand, when $L_i \neq 0$, an effective coupling between nonpolar and polar modes appears through a term $(F_1 L_2 + F_2 L_1) Q_a Q_1 Q_2$ in the adiabatic potential energy $\mathcal{E}$. As a consequence, all distortion modes are found to be nonzero at energy minima, thus implying that a polar displacement is always symmetry allowed, as shown in Fig. 1; at the same time, JT split states display an asymmetric mixing of d_{yz} and d_{zx}. Furthermore, the switching of Q_2 (hence of the local dipole) implies a change of sign of the product $Q_a Q_1$, consistently with the trilinear term coupling the two nonpolar and the polar modes. As a consequence, the energy barrier related to the dipole switching can in principle be much reduced with respect to the case of a single-mode instability [see, e.g., Fig. 1(d)].

III. JAHN-TELLER EFFECT IN $Ba_2NiGe_2O_7$

On the basis of the previous general analysis, we consider a hypothetical melilite oxide hosting JT-active T ions, where the polar JT effect previously discussed is expected to appear. We performed DFT calculations resorting to the VASP code [33] within the framework of the generalized gradient approximation adopting the Perdew-Burke-Enzerhof functional (GGA-PBE), while the electronic correlation has been also taken into account by using the GGA+U potential [34] (with $U = 2, 4$ or 6 eV for T ions). Electric polarization has been evaluated in the framework of the Berry-phase approach [35]. We started from the experimental crystal structure of $Ba_2CoGe_2O_7$ belonging to the $P\bar{4}2_1m$ space group [36] and fully optimized it by substituting Co with the JT-active ion Ni^{2+} while imposing different magnetic configurations of the transition-metal magnetic moments. We also considered V^{2+}, whose electronic configuration is physically equivalent to Ni^{2+}, but with occupied majority spins only. Indeed, results for both systems show qualitatively the same behavior, therefore we discuss here only the case of $Ba_2NiGe_2O_7$ (BNGO).

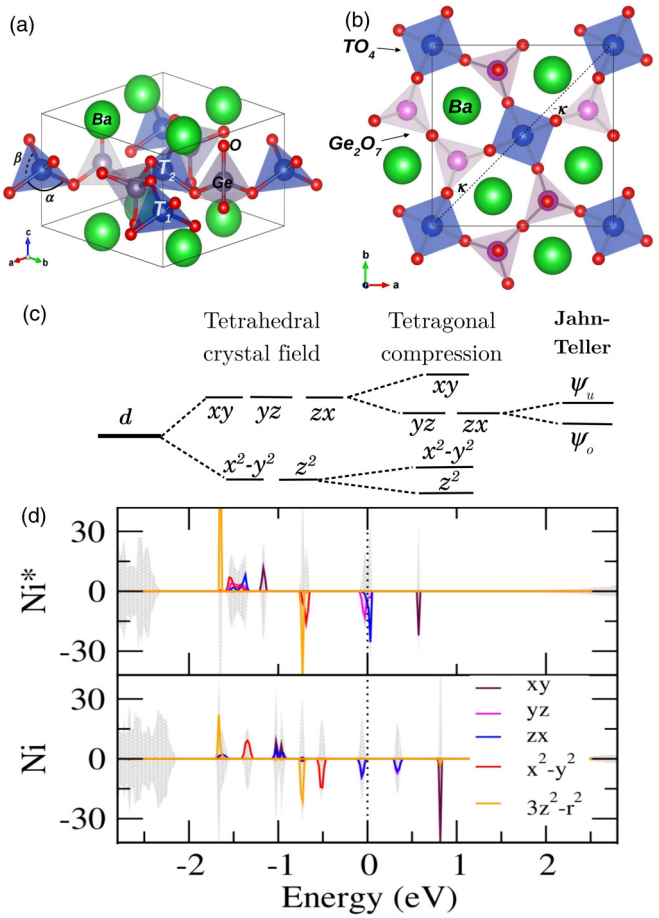

FIG. 2. (Color online) (a) Melilite crystal structure of $Ba_2TGe_2O_7$ with $P\bar{4}2_1m$ symmetry, showing layers of Ge_2O_7 dimers linked by TO_4 tetrahedra intercalated by Ba ions. The TO_4 tetrahedra are compressed along the c axis, resulting in different O-T-O angles α,β. (b) Top view of the crystal structure, highlighting two inequivalent TO_4 tetrahedra which are rotated about the c axis of $\pm\kappa$, respectively. (c) Level structure of the T^{2+} metal ion in the melilite crystal. In the tetrahedral environment, d orbitals split into lower e_g and higher t_{2g} manifolds; a tetragonal compression further splits the e_g,t_{2g} levels, leaving only twofold degenerated d_{yz},d_{zx} states. If these levels are half occupied, as in the case of Ni(d^8) or V(d^3), a JT distortion can take place, removing the only degeneracy left between the d_{yz} and d_{zx} states. (d) Density of states (states/eV) decomposed into d-orbital states and calculated within the bare GGA approach. "Ni*" refers to the parent-compound structure, belonging to space group $P\bar{4}2_1m$, while the optimized distorted structure with $Cmm2$ symmetry is labeled by "Ni."

In Fig. 2(d), we show the density of states of BNGO decomposed into d-orbital states, as obtained when a C -type antiferromagnetic configuration is imposed (similar results are obtained with other higher-energy magnetic configurations). When keeping the same space group $P\bar{4}2_1m$ of the parent compound, BNGO clearly shows a metallic behavior, arising from the twofold degeneracies of (d_{yz},d_{zx})-orbital states which are half filled in the minority spin manifold of $Ni^{2+}(d^8)$, being $e_g^{\uparrow 2}t_{2g}^{\uparrow 3}e_g^{\downarrow 2}t_{2g}^{\downarrow 1}$. The degeneracy can then be lifted by a JT structural distortion; indeed, we found that lowering the symmetry to the c-centered $Cmm2$ space group leads to the

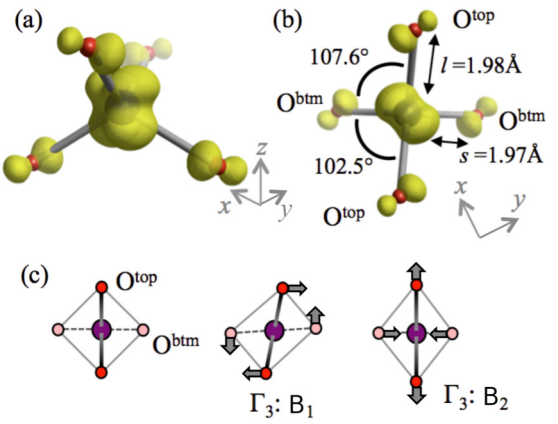

FIG. 3. (Color online) Charge density plot (obtained within the GGA+U approach, with $U = 4$ eV) corresponding to the highest occupied state of the Ni-d state hybridizing with tetrahedral O-p states, (a) in perspective view in a local xyz frame and (b) projected onto the xy plane. (c) Distortion modes of tetrahedral O ions surrounding the Ni ion, projected onto the xy plane, as obtained using the ISODISTORT program [37].

opening of an energy gap in the BNGO compound, which is $E_g = 0.3(2.3)$ eV at the bare GGA (GGA+U,$U = 4$ eV) level, with a corresponding total energy gain of 78(753) meV per formula unit (f.u.). We notice that the main effect of a finite U in the GGA+U approach is to induce a larger gap and a larger energy gain associated to the structural transition. Both the Ni-O bond lengths and O-Ni-O bond angles are differentiated, as shown in Fig. 3(b). Two short s (long l) bonds can be identified, linking the Ni ion with upper (lower) lying oxygens in the tetrahedral cage, which are $s = 1.95$ Å and $l = 2.00$ Å ($s = 1.97$ Å,$l = 1.98$ Å for $U = 4$ eV). Furthermore, the O^{top}-Ni-O^{btm} bond angles β, comprising upper- and lower-lying oxygens, differentiate in $\beta' = 106.1°$ (107.6° for $U = 4$ eV) and $\beta'' = 103.0°$ (102.5° for $U = 4$ eV), suggesting that the JT-induced distortions do not consist only in a Ni off-centering. Indeed, the ionic displacement from the $P\bar{4}2_1m$ to the $Cmm2$ structure can be decomposed [37] into a totally symmetric Γ_1 mode, with total amplitude $Q_{\Gamma_1} = 0.02$ Å, and a distortional (nontotally symmetric) mode, with total amplitude $Q_{\Gamma_3} = 0.13$ Å . The latter displacement mode can be further decomposed in two modes belonging to B_1 and B_2 symmetry representations, shown in Fig. 3(c) and corresponding to those shown in Figs. 1(g) and 1(h), in perfect agreement with our previous qualitative analysis. These modes display significant ionic displacements of O ions around the Ni cation, which are $Q_{B_1} = -0.10$ Å and $Q_{B_2} = 0.05$ Å . Upon structural distortion, the degenerate yz,zx states are split into occupied $0.61|yz\rangle - 0.79|zx\rangle$ and unoccupied $0.79|yz\rangle + 0.61|zx\rangle$ states, implying a mixing angle $\varphi = 37.7°$. From the point of view of structural distortions, the B_1 mode, differentiating both the bond angle and the bond length, appears as the largest JT mode; however, the electronic mixing angle appears closer to the value $\varphi_a = \pi/4$ of case a, suggesting that indeed the leading JT distortion arises from mode B_2, which is mainly responsible for the d-orbital state splitting. On the other hand, the simultaneous activation of both B_1 and B_2 modes, alongside the nonzero

amplitude of the totally symmetric displacement, points to non-negligible quadratic couplings L_i, which is further confirmed by the asymmetric mixing of the d_{yz}- and d_{zx}-orbital states.

IV. MULTIFERROICITY IN JAHN-TELLER MELILITES

If, on the one hand, the appearance of local dipoles in the TO_4 cage can be understood in terms of the JT effect, on the other hand, the onset of an ordered ferroelectric (FE) or antiferroelectric (AFE) phase is related to nonlocal interactions between the different tetrahedral units. Since there are two TO_4 tetrahedra in the parent unit cell, two possible structural configurations can be considered which realize the previously discussed local JT effect: (i) both T ions off center downward or upward (FE, $P_c \gtrless 0$, space group $Cmm2$), and (ii) T ions off center in opposite directions (AFE, $P_c = 0$, space group $P2_12_12_1$). As listed in Table I, the AFE structure in both compounds is energetically more stable by 20–30 meV/f.u. The antiferroelectric character of the cooperative JT interactions can be qualitatively understood in terms of the local coupling between on-site JT distortions. In fact, the sign of the polar distortion Q_2 is determined by the product Q_aQ_1, where the first nonpolar distortional mode is associated with a global rotation of the tetrahedral unit and the second to the antiphase rotation of O^{top} and O^{btm} around the tetrahedral z axis, as shown in Figs. 1(f) and 1(g), respectively. The sign of Q_a is opposite in the two TO_4 units, which are rotated by an angle $\pm\kappa$ in the melilite crystal; on the other hand, Q_1 is expected to display the same sign, in order to minimize the energetic cost associated with distortions of the Ge_2O_7 dimers linking the JT-active units by inducing less asymmetric changes of the O-Ge-O bond angles. The opposite sign of Q_aQ_1 thus may explain the observed antiferroelectric configurations of local dipoles associated with the Q_2 local modes. However, one can resort to a different JT ion occupying the T sites, such as V^{2+}. Indeed, when combining V and Ni ions, each carrying a different electric dipole, a ferrielectric configuration can be expected, as we show in Table I. On the other hand, the substantially local mechanism leading to the formation of electric dipoles suggests that ferroelectric behavior could be in principle attained when doping melilite oxides with JT-active ions; indeed, good-quality crystals of $Ba_2Cu_{1-x}Ni_xGe_2O_7$ have been successfully synthesized up to Ni concentrations of $x = 0.5$, with their structural and magnetic characterizations being under way [38,39].

TABLE I. Relative GGA+U ($U = 4$ eV) total energies and bulk polarization for paraelectric metallic (PE), FE, and AFE configurations in BNGO, $Ba_2VGe_2O_7$ (BVGO), and an ordered half-doped $Ba_2V_{0.5}Ni_{0.5}Ge_2O_7$ [B(V,N)GO] hypothetical compound, where the parallel (antiparallel) configuration of inequivalent electric dipoles results in a strong (weak) FE phase.

		ΔE (meV/f.u.)	P_c (μC/cm^2)
BNGO	PE	775.9	
	FE	22.9	1.18
	AFE	0	0
BVGO	PE	675.3	
	FE	30.3	1.90
	AFE	0	0
B(V,N)GO	PE	339.7	
	Strong FE	189.7	− 10.85
	Weak FE	0	0.70

As for the magnetic properties, we found that both Ni and V oxides display an antiferromagnetic ground state, and therefore they can be considered as proper multiferroic materials. The in-plane exchange constant J_{ab} appears to be the dominant antiferromagnetic interaction, while the out-of-plane exchange J_c changes from a ferro- to antiferromagnetic interaction when Ni is replaced by V, leading to C -type and G -type AFM configurations, respectively. In both cases, the estimated exchange anisotropy is rather strong, being $J_c/J_{ab} \lesssim 0.05$, thus displaying the quasi-2D character observed in known parent compounds. On the other hand, the most important contribution to the local spin-dependent hybridization mechanism mediating the reported large ME interaction in melilite oxides has been shown to arise from the d_{yz},d_{zx}-orbital states of the T ions [14]. Since these states are partially filled in JT melilites, a significant spin-dependent modulation of charge density at the lower- and upper-lying O ions through the asymmetric pd hybridization is expected to further contribute to the local electronic polarization, i.e., to mediate a ME interaction. Due to the partial occupancy of the active d states of T ions, such a ME interaction can be in principle of the same order of magnitude as that predicted for Co and Cu compounds, if not larger. Even though the relatively weak exchange interactions are responsible for very low Néel temperatures, signatures of such a ME coupling are expected to be visible even in the paramagnetic phase, due to the localized nature of its microscopic origin.

V. CONCLUSIONS

By combining symmetry-based JT analysis and DFT calculations, we put forward a mechanism for multiferroicity and theoretically predict the possibility of realizing proper FE and AFE phases in melilite oxides. We have shown that JT instabilities of noncentrosymmetric units can lead to polar distortions and possibly mediate a (anti)ferroelectric transition of proper character which could be signaled by large anomalies in the dielectric susceptibility. The cooperative JT origin of such a structural transition is also known to lead to enhanced electrostrictive and magnetostrictive responses that are expected to develop even if the predicted JT distortions display a dynamical, rather than static, character [24]. Remarkably, the JT polar distortions can be realized in the presence of a magnetic phase, thus circumventing the empirical exclusion rule between magnetism and ferroelectricity usually invoked for perovskite oxides. On the other hand, due to the proper nature of the predicted structural distortions, they are expected to take place at higher temperatures than those typically found for magnetically induced improper ferroelectrics, at the same time displaying an intrinsic ME interaction of local origin that could be detectable even above the magnetic transition temperature.

ACKNOWLEDGMENTS

P.B. thanks Dr. R. Fittipaldi and Dr. A. Vecchione for useful and fruitful discussions. This work has been supported by CNR-SPIN Seed Project PAQSE002 and MIUR-PRIN Project "Interfacce di ossidi: nuove proprietà emergenti, multifunzionalità e dispositivi per l'elettronica e l'energia" (OXIDE). DFT calculations were performed using the facilities of the Super Computer Center, the Institute for Solid State Physics, the University of Tokyo.

[1] *Colossal Magnetoresistive Manganites*, edited by T. Chatterji (Springer, Berlin, 2004).

[2] *Vibronic Interactions: Jahn-Teller Effect in Crystal and Molecules*, edited by M. D. Kaplan and G. O. Zimmerman, Nato Science Series II, Vol. 39 (Springer, Berlin, 2000).

[3] *The Jahn-Teller Effect*, edited by H. Köppel, D. R. Yarkony, and H. Barentzen, Springer Series in Chemical Physics Vol. 97 (Springer, Berlin, 2010).

[4] I. B. Bersuker, *The Jahn-Teller Effect* (Cambridge University Press, Cambridge, U.K., 2006).

[5] J. M. Rondinelli, A. S. Eidelson, and N. A. Spaldin, Non-d_0 Mn-driven ferroelectricity in antiferromagnetic $BaMnO_3$, Phys. Rev. B **79**, 205119 (2009).

[6] S. Bhattacharjee, E. Bousquet, and P. Ghosez, Engineering multiferroism in $CaMnO_3$, Phys. Rev. Lett. **102**, 117602 (2009).

[7] P. Barone, S. Kanungo, S. Picozzi, and T. Saha-Dasgupta, Mechanism of ferroelectricity in d_3 perovskites: A model study, Phys. Rev. B **84**, 134101 (2011).

[8] I. B. Bersuker, Pseudo Jahn-Teller origin of perovskite multiferroics, magnetic-ferroelectric crossover, and magnetoelectric effects: The d_0-d_{10} problem, Phys. Rev. Lett. **108**, 137202 (2012).

[9] N. A. Hill, Why are there so few magnetic ferroelectrics? J. Phys. Chem. B **104**, 6694 (2000).

[10] T. Arima, Ferroelectricity induced by proper-screw type magnetic order, J. Phys. Soc. Jpn. **76**, 073702 (2007).

[11] C. Jia, S. Onoda, N. Nagaosa, and J. H. Han, Microscopic theory of spin-polarization coupling in multiferroic transition metal oxides, Phys. Rev. B **76**, 144424 (2007).

[12] H. Murakawa, Y. Onose, S. Miyahara, N. Furukawa, and Y. Tokura, Ferroelectricity induced by spin-dependent metal-ligand hybridization in $Ba_2CoGe_2O_7$, Phys. Rev. Lett. **105**, 137202 (2010).

[13] H. J. Xiang, E. J. Kan, Y. Zhang, M.-H. Whangbo, and X. G. Gong, General theory for the ferroelectric polarization induced by spin-spiral order, Phys. Rev. Lett. **107**, 157202 (2011).

[14] K. Yamauchi, P. Barone, and S. Picozzi, Theoretical investigation of magnetoelectric effects in $Ba_2CoGe_2O_7$, Phys. Rev. B **84**, 165137 (2011).

[15] K. Yamauchi, T. Oguchi, and S. Picozzi, Ab-initio prediction of magnetoelectricity in infinite-layer $CaFeO_2$ and $MgFeO_2$, J. Phys. Soc. Jpn. **83**, 094712 (2014).

[16] H. Murakawa, Y. Onose, S. Miyahara, N. Furukawa, and Y. Tokura, Comprehensive study of the ferroelectricity induced by the spin-dependent *d-p* hybridization mechanism in $Ba_2XGe_2O_7$ (X = Mn, Co, and Cu), Phys. Rev. B **85**, 174106 (2012).

[17] M. Akaki, J. Tozawa, D. Akahoshi, and H. Kuwahara, Magnetic and dielectric properties of $A_2CoSi_2O_7$ (A = Ca, Sr, Ba) crystals, J. Phys.: Conf. Ser. **150**, 042001 (2009).

[18] M. Akaki, H. Iwamoto, T. Kihara, M. Tokunaga, and H. Kuwahara, Multiferroic properties of an åkermanite $Sr_2CoSi_2O_7$ single crystal in high magnetic fields, Phys. Rev. B **86**, 060413(R) (2012).

[19] A. Zheludev, G. Shirane, Y. Sasago, N. Koide, and K. Uchinokura, Spiral phase and spin waves in the quasi-two-dimensional antiferromagnet $Ba_2CuGe_2O_7$, Phys. Rev. B **54**, 15163 (1996).

[20] A. N. Bogdanov, U. K. Roßler, M. Wolf, and K.-H. Müller, Magnetic structures and reorientation transitions in noncentrosymmetric uniaxial antiferromagnets, Phys. Rev. B **66**, 214410 (2002).

[21] H. T. Yi, Y. J. Choi, S. Lee, and S.-W. Cheong, Multiferroicity in the square-lattice antiferromagnet of $Ba_2CoGe_2O_7$, Appl. Phys. Lett. **92**, 212904 (2008).

[22] S. Bordács, I. Kézsmárki, D. Szaller, L. Demkóó, N. Kida, H. Murakawa, Y. Onose, R. Shimano, T. Rõõm, U. Nagel, S. Miyahara, N. Furukawa, and Y. Tokura, Chirality of matter shows up via spin excitations, Nat. Phys. **8**, 734 (2013).

[23] I. Kézsmárki, N. Kida, H. Murakawa, S. Bordács, Y. Onose, and Y. Tokura, Enhanced directional dichroism of terahertz light in resonance with magnetic excitations of the multiferroic $Ba_2CoGe_2O_7$ oxide compound, Phys. Rev. Lett. **106**, 057403 (2011).

[24] M. D. Kaplan and B. G. Vekhter, *Cooperative Phenomena in Jahn-Teller Crystals* (Plenum, New York, 1995).

[25] L. N. Pelikh and A. A. Gurskas, Jahn-Teller phase transition in $KDy(WO_4)_2$, Fiz. Tverd. Tela (Leningrad) **21**, 2136 (1979) [Sov. Phys. Solid State **21**, 1223 (1979)].

[26] B. G. Vekhter and M. D. Kaplan, Connection between the anomalies of the elastic and dielectric characteristics of the Jahn-Teller crystal $DyVO_4$, Sov. Phys. JETP **51**, 893 (1980).

[27] M. J. M. Leask, A. C. Tropper, and M. R. Wells, Antiferrodistortive Jahn-Teller ordering in $KDy(MoO_4)_2$, J. Phys. C: Solid State Phys. **14**, 3481 (1981).

[28] H. Unoki and T. Sakudo, Dielectric anomaly and improper antiferroelectricity at the Jahn-Teller transitions in rare-earth vanadates, Phys. Rev. Lett. **38**, 137 (1977).

[29] K. Kishimoto, T. Ishikura, H. Nakamura, Y. Wakabayashi, and T. Kimura, Antiferroelectric lattice distortion induced by ferroquadrupolar order in $DyVO_4$, Phys. Rev. B **82**, 012103 (2010).

[30] J. P. Harrison, J. P. Hessler, and D. R. Taylor, One- and three-dimensional antiferroelectric ordering in $PrCl_3$, Phys. Rev. B **14**, 2979 (1976).

[31] D. R. Taylor, J. P. Harrison, and D. B. McColl, Co-operative Jahn-Teller ordering in praseodymium compounds, Physica B+C **86–88**, 1164 (1977).

[32] U. Öpik and M. H. L. Pryce, Studies of the Jahn-Teller effect. I. A survey of the static problem, Proc. R. Soc. London, Ser. A **238**, 425 (1957).

[33] G. Kresse and J. Furthmüller, Efficient iterative schemes for ab initio total-energy calculations using a plane-wave basis set, Phys. Rev. B **54**, 11169 (1996).

[34] V. I. Anisimov, F. Aryasetiawan, and A. I. Lichtenstein, First-principles calculations of the electronic structure and spectra of strongly correlated systems: The LDA+U method, J. Phys.: Condens. Matter **9**, 767 (1997).

[35] R. D. King-Smith and D. Vanderbilt, Theory of polarization of crystalline solids, Phys. Rev. B **47**, 1651 (1993); R. Resta, Macroscopic polarization in crystalline dielectrics: The geometric phase approach, Rev. Mod. Phys. **66**, 899 (1994).

[36] V. Hutanu, A. Sazonov, H. Murakawa, Y. Tokura, B. Náfrádi, and D. Chernyshov, Symmetry and structure of multiferroic $Ba_2CoGe_2O_7$, Phys. Rev. B **84**, 212101 (2011).

[37] B. J. Campbell, H. T. Stokes, D. E. Tanner, and D. M. Hatch, ISODISPLACE: A web-based tool for exploring structural distortions, J. Appl. Crystallogr. **39**, 607 (2006).

[38] R. Fittipaldi, L. Rocco, M. Ciomaga Hatnean, V. Granata, M. R. Lees, G. Balakrishnan, and A. Vecchione, Crystal growth and characterization of the non-centrosymmetric antiferromagnet $Ba_2CoGe_2O_7$, J. Cryst. Growth **404**, 223 (2014).

[39] R. Fittipaldi, L. Rocco, V. Granata, and A. Vecchione (private communication).